

# VARIABILITY OF FUNCTIONAL CONNECTOMES THROUGH COMMUNITY STRUCTURE

Brooke Osterkamp, Meiby Ortiz-Bouza, and Selin Aviyente

Department of Electrical and Computer Engineering, Michigan State University  
East Lansing, 48824  
aviyente@egr.msu.edu

## ABSTRACT

Traditional neuroimaging research typically focuses on identifying group level characteristics of brain connectivity across subjects. However, recent research has shown that even among the neurologically healthy, brain function shows high individual variability. This realization has lead to the concept of functional connectome (FC) fingerprinting, where the functional connectivity profiles act as a fingerprint that can be used to identify the individual and establish a relationship between brain function and behavior. A core component of fingerprinting is feature selection where a subset of edges from FC are selected. In this paper, we propose an alternative feature selection approach where functional subnetworks instead of individual edges are identified to describe group and individual level network activity. The proposed approach models the FCs from multiple subjects as a multiplex network and employs a community detection method to extract functional subnetworks that are common and unique across subjects. We then introduce metrics to evaluate the common communities and quantify their consistency and variability across subjects. The proposed framework is evaluated on functional connectomes constructed from electroencephalogram (EEG) data during a cognitive control study.

**Index Terms**— Functional Connectome, Community Detection, Individual Variability, Electroencephalogram

## 1. INTRODUCTION

Over the past two decades, there has been a growing interest in the study of functional connectivity in the brain from different imaging modalities such as the functional magnetic resonance imaging (fMRI), electroencephalography (EEG), and magnetoencephalography (MEG) [1]. While different methods have been proposed to quantify functional connectivity, the research community has not reached a consensus on how to evaluate the resulting functional connectomes (FCs) within and across a group of subjects.

The first class of methods focus on inferring group level characteristics of FCs. One such approach has been to analyze the networks estimated from brain-imaging modalities by means of graph theoretic tools [2, 3]. Graph theory provides mathematical tools for extracting features that could concisely describe the structure of the estimated cerebral networks. This class of methods usually extract graph theoretic metrics such as the clustering coefficient, efficiency and small-world parameter. These metrics are then compared between groups using statistical testing. While this approach is effective at summarizing the network activity at the group level and discriminating between subject groups, it cannot identify the local network components that contribute to the observed differences.

This work was supported in part by the NSF under CCF-2006800.

Another class of methods in this category rely on extracting low-dimensional latent embeddings such as group independent component analysis (GICA) and group information guided ICA (GIG-ICA) [4, 5]. These methods enable the extraction of intrinsic connectivity patterns at both the group and subject-level.

While group-level inferences inform us of the generic principles, they obscure principles specific to individual subjects that are essential for characterizing brain function in health and disease. Recently, functional connectome fingerprinting [6], where the goal is to uniquely identify individual subjects using subject-specific FC, has gained a lot of attention. Specifically, given a set of  $N$  reference fMRI scans, one from each of the  $N$  subjects, and a new target fMRI scan from one of the same  $N$  subjects, the goal is to identify the subject by “matching” the functional connectome of the target scan with that of the reference scans. A variety of methods for performing fingerprinting using FC have been developed since this initial work. These methods either use the whole connectivity matrix or pre-defined subnetworks to identify individual subjects [7]. More recently, feature extraction methods such as PCA [8], graph embedding based approach [9] and deep learning-based approaches [10] have been proposed for fingerprinting. While these methods have been successful in accurately identifying subjects from their FC profiles, they have some shortcomings. First, simple fingerprinting methods use either the whole FC or individual edges and thus cannot identify functionally meaningful network components that contribute most to individuality. Second, the more advanced feature extraction methods do not necessarily produce interpretable features limiting their use in neuroimaging. Finally, current methods mostly focus on accuracy of subject identification rather than characterizing both group and subject-level network components of FC.

In this paper, we aim to fill these gaps by introducing a network based approach to characterize FCs. First, we propose to model the FCs across multiple subjects as a multiplex network where each layer corresponds to the FC of an individual [11, 12]. We then adopt a recently introduced community detection algorithm [13] to identify both common and individual communities across subjects. This approach enables us to take the heterogeneity of FCs across a group of subjects into account. The resulting communities are then evaluated based on their consistency and variability within a group.

## 2. BACKGROUND

### 2.1. Community Detection

A graph can be represented as  $\mathcal{G} = \{V, E, \mathbf{A}\}$ , where  $V$ ,  $E$  and  $\mathbf{A}$  are the set of nodes, edges, and adjacency matrix of the graph, respectively. Community detection refers to the task of partitioning the node set  $V$  as  $\mathcal{C} = \{C_1, \dots, C_P\}$ , where  $P$  denotes the number of communities. One widely used method for partitioning graphs is

the minimum cut approach, including the ratio cut and normalized cut [14]. These methods aim to partition the graph such that the number of edges between different communities is minimized.

For a given graph, the min-cut problem finds a partition that minimizes the following objective function:

$$\frac{1}{2} \sum_{p=1}^K \mathbf{Cut}(C_p, \bar{C}_p), \quad (1)$$

where  $\bar{C}_p$  represents the complement of  $C_p$  and  $\mathbf{Cut}(C_p, \bar{C}_p)$  is the sum of the edge weights between two disjoint sets  $C_p$  and  $\bar{C}_p$ . The min-cut problem is NP-hard, but it has been shown that spectral clustering and non-negative matrix factorization provide solutions to relaxed versions of this problem [14, 15].

In [15], it was shown that normalized cut using the normalized adjacency matrix,  $\tilde{\mathbf{A}} = \mathbf{D}^{-1/2} \mathbf{A} \mathbf{D}^{-1/2}$ , where  $\mathbf{D}$  is the degree matrix defined as  $D_{ii} = \sum_j A_{ij}$ , is equivalent to the nonnegative matrix factorization problem with  $\underset{\mathbf{H} \geq 0}{\operatorname{argmin}} \|\tilde{\mathbf{A}} - \mathbf{H} \mathbf{H}^\top\|^2$ .

## 2.2. Multiplex Networks

Multiplex networks are high-dimensional networks composed of multiple layers, where each layer shares the same set of nodes with edges varying across layers. A sequence of graphs  $\mathcal{G}_l = (V_l, E_l, \mathbf{A}_l)$ , with  $l \in \{1, 2, \dots, L\}$  is used to represent multiplex networks [16]. Here,  $V_l$  denotes the set of nodes in layer  $l$ ,  $E_l$  is the set of edges and  $\mathbf{A}_l \in \mathbb{R}^{n \times n}$  represents the adjacency matrix for layer  $l$ . In this paper, we consider undirected weighted adjacency matrices with  $A_{l_{ij}} \in [0, 1]$ .

## 2.3. Functional Connectome Construction

A weighted graph can be constructed from EEG signals with the nodes corresponding to brain regions and the edge weights corresponding to functional connectivity. In this paper, we use a time-frequency based phase synchrony measure to quantify functional connectivity [17]. The Phase Locking Value (PLV) between two signals  $x_i$  and  $x_j$  as a function of time and frequency [18] is defined as

$$PLV_{i,j}(t, \omega) = \frac{1}{N} \left| \sum_{k=1}^N \exp \left( j\Phi_{i,j}^k(t, \omega) \right) \right|, \quad (2)$$

where  $N$  is the number of trials and  $\Phi_{i,j}^k(t, \omega)$  is the phase difference between  $x_i^k$  and  $x_j^k$  defined as  $\Phi_{i,j}^k(t, \omega) = \arg \left[ \frac{C_i^k(t, \omega)}{|C_i^k(t, \omega)|} \frac{C_j^{k*}(t, \omega)}{|C_j^k(t, \omega)|} \right]$  for the  $k^{\text{th}}$  trial with  $C_i^k(t, \omega)$  being the RID-Rihaczek time-frequency distribution [19].

The adjacency matrix for each subject,  $l$ , is then constructed as the average phase locking value within a time window,  $T$ , and frequency band,  $\Omega$ , of interest as  $\mathbf{A}_l(i, j) = \frac{1}{|T||\Omega|} \sum_{t \in T} \sum_{\omega \in \Omega} PLV(t, \omega)$ .

## 3. METHOD

### 3.1. Multiplex Community Detection Based on Orthogonal Nonnegative Matrix Trifactorization (MX-ONMTF)

In this paper, we use MX-ONMTF [13], a multiplex community detection method that models each layer's adjacency matrix as the sum of low-rank representations of common and private communities using Orthogonal Nonnegative Matrix Tri-Factorization (ON-MTF). For a multiplex network with  $L$  layers and adjacency ma-

trices,  $\mathbf{A}_l \in \mathbb{R}^{n \times n}$ ,  $l \in \{1, 2, \dots, L\}$ , the objective function is formulated as

$$\begin{aligned} \underset{\mathbf{H} \geq 0, \mathbf{H}_l \geq 0, \mathbf{S}_l \geq 0, \mathbf{G}_l \geq 0}{\operatorname{argmin}} \sum_{l=1}^L \|\mathbf{A}_l - \mathbf{H} \mathbf{S}_l \mathbf{H}^\top - \mathbf{H}_l \mathbf{G}_l \mathbf{H}_l^\top\|_F^2 \\ \text{s.t. } \mathbf{H}^\top \mathbf{H} = \mathbf{I}, \mathbf{H}_l^\top \mathbf{H}_l = \mathbf{I}, \text{ with } l \in \{1, 2, \dots, L\}, \end{aligned} \quad (3)$$

where  $\mathbf{H} \in \mathbb{R}^{n \times k_c}$  and  $\mathbf{H}_l \in \mathbb{R}^{n \times k_{p_l}}$ , are the community membership matrices corresponding to the common and private communities, respectively, and  $\mathbf{S}_l \in \mathbb{R}^{k_c \times k_c}$  and  $\mathbf{G}_l \in \mathbb{R}^{k_{p_l} \times k_{p_l}}$  are symmetric matrices that capture the inter-community interactions and provide additional degrees of freedom.

ONMTF optimization problem in (3) can be solved using a multiplicative update algorithm (MUA) similar to [20]. MX-ONMTF follows this approach to derive the multiplicative update rules for each variable as given in [13]. Algorithm 1 shows an overview of the method. The algorithm converges when the norms of the difference between two consecutive updates of all the variables are less than a pre-determined threshold, e.g.,  $\|\mathbf{H}^{(k)} - \mathbf{H}^{(k+1)}\|_F^2 \leq \epsilon$ . Then, the community label of each node is found by identifying the column of  $[\mathbf{H}, \mathbf{H}_l]$  with the highest value for each row.

---

### Algorithm 1 MX-ONMTF

---

**Input:** Adjacency matrices  $\mathbf{A}_l$ ,  $l \in \{1, 2, \dots, L\}$ .  
**Output:** Community membership matrices  $\mathbf{H}$ ,  $\mathbf{H}_l$ .

- 1: Find  $k_c$ ,  $k_l$ , and  $k_{p_l}$  using Algorithm 2 in [13].  $k_l$ 's are found using the eigengap rule for each layer.  $k_c$  is found by applying ONMTF to each layer and using agglomerative hierarchical clustering across the low-dimensional embeddings of each layer.
- 2: **for**  $r=1$  to  $50$  **do**
- 3:   Randomly initialize  $\mathbf{H}$ ,  $\mathbf{H}_l$ ,  $\mathbf{S}_l$ ,  $\mathbf{G}_l > 0$
- 4:   **for** 1000 iterations or until convergence **do**
- 5:     update  $\mathbf{H}$ ,  $\mathbf{H}_l$ ,  $\mathbf{S}_l$ , and  $\mathbf{G}_l$  using their corresponding multiplicative updates.
- 6:   **end for**
- 7:   **for** each layer  $l$  **do**
- 8:     Identify which common communities are present in each layer  $l$  using Algorithm 3 in [13].
- 9:     **for** each  $i$  **do**
- 10:        $\mathbf{H}_{l_{new}} = [\mathbf{H}, \mathbf{H}_l]$
- 11:        $idx \leftarrow \operatorname{argmax}_j \mathbf{H}_{l_{new}}(i, j)$
- 12:       **if**  $idx(i) > k_c$  **then**
- 13:            $idx(i) \leftarrow (\operatorname{argmax}_j \mathbf{H}_{l_{new}}(i, j)) + \sum_{n=1}^{l-1} k_{p_n}$
- 14:       **end if**
- 15:     **end for**
- 16:   **end for**
- 17:   Compute the modularity density,  $Q_{Dr}$ , [21].
- 18: **end for**
- 19: Choose the partition  $r^* = \operatorname{argmax}_r Q_{Dr}$ .

---

### 3.2. Consistency

Once the  $k_c$  common communities are identified, we quantify the consistency of each brain region across subjects. For this purpose, we introduce a measure of consistency of a node  $i$  with respect to each of the  $k_c$  communities as follows:

$$C_i^k = \frac{\mathbf{H}(i, k)}{\sum_{k=1}^{k_c} \mathbf{H}(i, k)}. \quad (4)$$

This metric quantifies the probability of node  $i$  appearing in the  $k$ th common community and is always between 0 and 1.

### 3.3. Variability

In addition to quantifying the importance of each node in describing the common community structure, we also quantify the variability of each common community across subjects. The variability is quantified by a measure of normalized intra-community strength which computes the ratio of the strength of intra-community edges to the total connectivity (strength) for a given FC. The variability of subject  $l$  with respect to the common community  $k$  is quantified as:

$$Var_l^k = \frac{\sum_{(i,j) \in C_k} \mathbf{A}_l(i,j)}{\sum_{i,j} \mathbf{A}_l(i,j)}. \quad (5)$$

This measure is also between 0 and 1 and quantifies how important common community  $k$  is with respect to each subject thus quantifying the variability in FC.

## 4. RESULTS

### 4.1. EEG Data

In this paper, we analyze EEG data collected during a cognitive control-related error processing study. The experimental procedures involving human subjects were approved by the MSU Institutional Review Board. All participants were female and the mean age was 20.78 (SD = 1.81). A letter version of the speeded reaction Flanker task [22] was performed. For each trial, a string of five letters, which could be congruent (e.g., SSSSS) or incongruent stimuli (e.g., SSTSS), were presented to each participant. The participants were instructed to select the center letter with a standard mouse with respect to the Flanker letters. Each trial began with 35ms of flanking stimuli (e.g., SS SS). After that, the target stimuli were presented for 100 ms (total presentation time is 135ms) by embedding them in the center of the flanker letters (e.g., SSSSS/SSTSS) followed by an inter-trial random interval ranging from 1200 to 1700 ms.

The EEG was recorded using the ActiveTwo system (BioSemi, Amsterdam, The Netherlands). 64 Ag-AgCl electrodes were placed following the international 10/20 system. The sampling frequency of the data was 512 Hz. Trials with artifacts were removed and Current Source Density (CSD) Toolbox [23] was used to minimize the volume conduction. Each trial was one second long. For the multi-subject FC analysis, the trials corresponding to the error responses from 20 participants were considered. The inclusion criterion was that the number of trials for error response should be at least 40.

### 4.2. Functional Connectomes

We are interested in studying the community structure in the FCs corresponding to error-related negativity (ERN) across subjects. ERN is an event-related brain potential following error responses. Previous studies have shown that the ERN is associated with increased synchronization in the theta band (4-8 Hz) between electrodes in the central and lateral frontal regions [22, 24]. FCs from error responses were constructed using the bivariate phase-locking value (PLV) between pairs of electrodes [19]. For each subject, a FC was constructed by averaging the PLV over the frequency bins corresponding to the theta band and the ERN time window, [0 – 100] ms.

The resulting FCs are fully connected and are not usually suitable for subsequent graph theoretic analysis. For this reason, thresholding is a commonly applied approach in functional connectomics

to remove spurious connections and to obtain sparsely connected matrices prior to graph theoretical analysis such as community detection. To avoid systematic differences in absolute number of edges, in this paper we use proportional thresholding with the threshold equal to 0.9, where a pre-defined number of strongest connections are selected as network edges, ensuring equal network density across datasets [25].

### 4.3. Community Structure Across Subjects

We applied the MX-ONMTF algorithm to a multiplex network of FCNS with  $L = 20$  and  $n = 64$  corresponding to the number of layers and brain regions. The number of communities was determined as 3 common communities across 20 subjects. The distribution of communities across layers is given in Fig. 1. From this figure, it can be seen that the first common community is present across 11 subjects, while the second and third common communities are present across 6 and 3 subjects, respectively. In addition to these common communities, 16 subjects each have one private community.

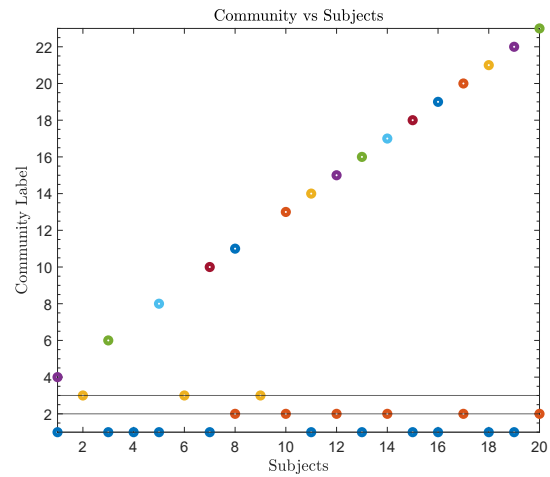


**Fig. 1:** Scatter plot of communities versus subjects

We analyzed the distribution of nodes or brain regions across subjects for the first two communities that account for the connectivity patterns in the majority of subjects. Common community 3 is not illustrated as it consists of all the nodes in the network and does not constitute an actual community. This community structure appears in 3 subjects which implies that for these subjects the connectivity values do not show significant variation resulting in a single large community. The consistency of each node within a community is computed using (4) and plotted in Fig. 2. From this figure, it can be seen that for the first community, the highly consistent nodes are concentrated around the medial prefrontal cortex (mPFC), e.g., FCz, FC2, FC4, and right lateral prefrontal cortex (IPFC), e.g., F6, F8. This is consistent with prior work on community structure associated with ERN and with the time-domain ERN component topographies [26]. In addition to this fronto-central structure, community 1 also contains nodes in the parietal and occipital areas as visual cortex is consistently recruited in response to the visual stimulus. Community 2, on the other hand, consists of nodes corresponding to the motor cortex, e.g., C2, CPz, as the task requires the subjects to make a motor response. This motor-related cluster structure was observed in prior research [26]. In addition to this cluster, community 2 also

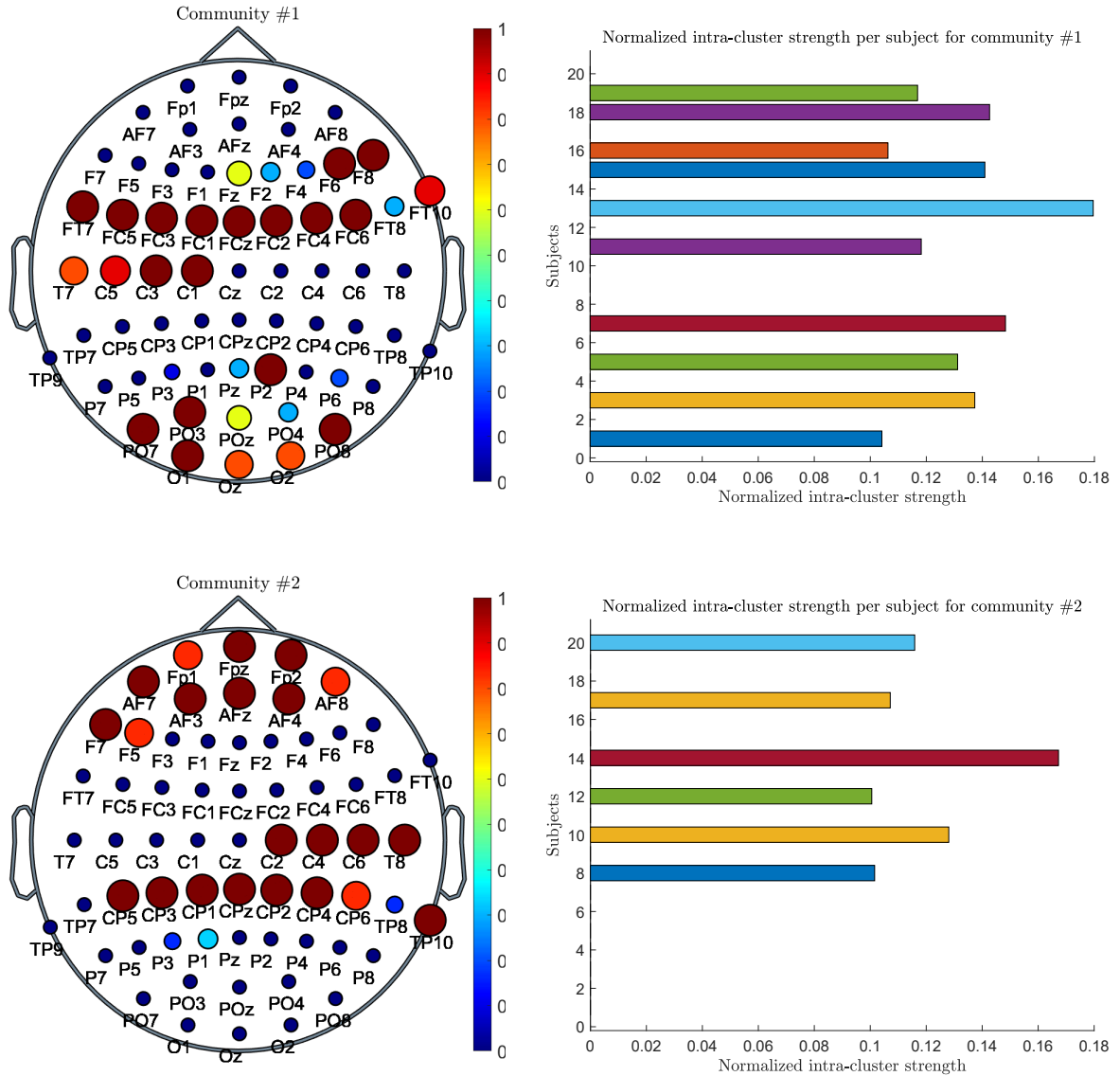


**Fig. 2:** Brain topomaps illustrating the consistency of each node with respect to the common communities and variability of the common communities across subjects. (Top) Common Community 1, (Bottom) Common Community 2.

contains nodes in the left and right-PFC.

The two common communities extracted from the 20 subjects are also analyzed with respect to their individuality or variability across subjects using the metric defined in (5). This metric shows how important a particular community is for a given subject. From Fig. 2, it can be seen that the common communities account for at least 10% of the total connectivity within each subject. There is considerable variability of the importance of these community structures across subjects.

## 5. CONCLUSIONS

In this paper, we introduced a multiplex network model to characterize variability of functional connectomes across a healthy group

of subjects performing the same task. In particular, a recently introduced multiplex community detection algorithm, MX-ONMTF, is adopted to determine functional subnetworks that are common and unique to each layer. We furthermore introduced measures of consistency and variability to identify brain regions that consistently play a functional role during ERN and quantify the variability of community structure across subjects.

Future work will consider extending this framework for FC fingerprinting applications. Unlike the majority of current fingerprinting methods which either focus on the whole brain connectivity or individual edges, the proposed framework provides interpretable functional subnetworks that can be used to identify subjects. Furthermore, these subnetworks can be used to construct behavior prediction models.

## 6. REFERENCES

- [1] André M Bastos and Jan-Mathijs Schoffelen, “A tutorial review of functional connectivity analysis methods and their interpretational pitfalls,” *Frontiers in systems neuroscience*, vol. 9, pp. 175, 2016.
- [2] Cornelis Jan Stam, Willem De Haan, ABFJ Daffertshofer, BF Jones, I Manshanden, Anne-Marie van Cappellen van Walsum, Teresa Montez, JPA Verbunt, Jan C De Munck, Bob Wilhelm Van Dijk, et al., “Graph theoretical analysis of magnetoencephalographic functional connectivity in alzheimer’s disease,” *Brain*, vol. 132, no. 1, pp. 213–224, 2009.
- [3] Ed Bullmore and Olaf Sporns, “Complex brain networks: graph theoretical analysis of structural and functional systems,” *Nature reviews neuroscience*, vol. 10, no. 3, pp. 186–198, 2009.
- [4] Vince D Calhoun, Jingyu Liu, and Tülay Adalı, “A review of group ica for fmri data and ica for joint inference of imaging, genetic, and erp data,” *Neuroimage*, vol. 45, no. 1, pp. S163–S172, 2009.
- [5] Yuhui Du and Yong Fan, “Group information guided ica for fmri data analysis,” *Neuroimage*, vol. 69, pp. 157–197, 2013.
- [6] Emily S Finn, Xilin Shen, Dustin Scheinost, Monica D Rosenberg, Jessica Huang, Marvin M Chun, Xenophon Papademetris, and R Todd Constable, “Functional connectome fingerprinting: identifying individuals using patterns of brain connectivity,” *Nature neuroscience*, vol. 18, no. 11, pp. 1664–1671, 2015.
- [7] Kendrick Li, Krista Wisner, and Gowtham Atluri, “Feature selection framework for functional connectome fingerprinting,” *Human Brain Mapping*, vol. 42, no. 12, pp. 3717–3732, 2021.
- [8] Enrico Amico and Joaquín Goñi, “The quest for identifiability in human functional connectomes,” *Scientific reports*, vol. 8, no. 1, pp. 8254, 2018.
- [9] Kausar Abbas, Enrico Amico, Diana Otero Svaldi, Uttara Tipnis, Duy Anh Duong-Tran, Mintao Liu, Meenusee Rajapandian, Jaroslaw Harezlak, Beau M Ances, and Joaquín Goñi, “Geff: Graph embedding for functional fingerprinting,” *NeuroImage*, vol. 221, pp. 117181, 2020.
- [10] Nicolás F Lori, Ivo Ramalhosa, Paulo Marques, and Victor Alves, “Deep learning based pipeline for fingerprinting using brain functional mri connectivity data,” *Procedia Computer Science*, vol. 141, pp. 539–544, 2018.
- [11] Federico Battiston, Vincenzo Nicosia, and Vito Latora, “The new challenges of multiplex networks: Measures and models,” *The European Physical Journal Special Topics*, vol. 226, pp. 401–416, 2017.
- [12] Meichen Yu, Marjolein MA Engels, Arjan Hillebrand, Elisabeth CW Van Straaten, Alida A Gouw, Charlotte Teunissen, Wiesje M Van Der Flier, Philip Scheltens, and Cornelis J Stam, “Selective impairment of hippocampus and posterior hub areas in alzheimer’s disease: an meg-based multiplex network study,” *Brain*, vol. 140, no. 5, pp. 1466–1485, 2017.
- [13] Meiby Ortiz-Bouza and Selin Aviyente, “Community detection in multiplex networks based on orthogonal nonnegative matrix tri-factorization,” *arXiv preprint arXiv:2205.00626*, 2022.
- [14] Ulrike Von Luxburg, “A tutorial on spectral clustering,” *Statistics and computing*, vol. 17, no. 4, pp. 395–416, 2007.
- [15] Chris Ding, Xiaofeng He, and Horst D Simon, “On the equivalence of nonnegative matrix factorization and spectral clustering,” in *Proceedings of the 2005 SIAM international conference on data mining*, pp. 606–610, 2005.
- [16] Emanuele Cozzo, Mikko Kivelä, Manlio De Domenico, Albert Solé-Ribalta, Alex Arenas, Sergio Gómez, Mason A Porter, and Yamir Moreno, “Structure of triadic relations in multiplex networks,” *New Journal of Physics*, vol. 17, no. 7, pp. 073029, 2015.
- [17] Selin Aviyente and Ali Yener Mutlu, “A time-frequency-based approach to phase and phase synchrony estimation,” *IEEE Transactions on Signal Processing*, vol. 59, no. 7, pp. 3086–3098, 2011.
- [18] Jean-Philippe Lachaux, Eugenio Rodriguez, Jacques Martinerie, and Francisco J Varela, “Measuring phase synchrony in brain signals,” *Human brain mapping*, vol. 8, no. 4, pp. 194–208, 1999.
- [19] Selin Aviyente, Edward M Bernat, Westley S Evans, and Scott R Sponheim, “A phase synchrony measure for quantifying dynamic functional integration in the brain,” *Tech. Rep.*, Wiley Online Library, 2011.
- [20] Chris Ding, Tao Li, Wei Peng, and Haesun Park, “Orthogonal nonnegative matrix t-factorizations for clustering,” in *Proceedings of the 12th ACM SIGKDD international conference on Knowledge discovery and data mining*, 2006, pp. 126–135.
- [21] Zhenping Li, Shihua Zhang, Rui-Sheng Wang, Xiang-Sun Zhang, and Luonan Chen, “Quantitative function for community detection,” *Physical review E*, vol. 77, no. 3, pp. 036109, 2008.
- [22] Tim P Moran, Ed M Bernat, Selin Aviyente, Hans S Schroder, and Jason S Moser, “Sending mixed signals: worry is associated with enhanced initial error processing but reduced call for subsequent cognitive control,” *Social cognitive and affective neuroscience*, vol. 10, no. 11, pp. 1548–1556, 2015.
- [23] Craig E Tenke and Jürgen Kayser, “Generator localization by current source density (csd): implications of volume conduction and field closure at intracranial and scalp resolutions,” *Clinical neurophysiology*, vol. 123, no. 12, pp. 2328–2345, 2012.
- [24] James F Cavanagh, Michael X Cohen, and John JB Allen, “Prelude to and resolution of an error: Eeg phase synchrony reveals cognitive control dynamics during action monitoring,” *Journal of Neuroscience*, vol. 29, no. 1, pp. 98–105, 2009.
- [25] Martijn P van den Heuvel, Siemon C de Lange, Andrew Zalesky, Caio Seguin, BT Thomas Yeo, and Ruben Schmidt, “Proportional thresholding in resting-state fmri functional connectivity networks and consequences for patient-control connectome studies: Issues and recommendations,” *Neuroimage*, vol. 152, pp. 437–449, 2017.
- [26] Alp Ozdemir, Marcos Bolanos, Edward Bernat, and Selin Aviyente, “Hierarchical spectral consensus clustering for group analysis of functional brain networks,” *IEEE Transactions on Biomedical Engineering*, vol. 62, no. 9, pp. 2158–2169, 2015.